Supporting Information

A Flexible Rechargeable Quasi-Solid-State Ni-Fe Battery Based on Surface Engineering Exhibits High Energy and Long Durability

Wenda Qiu*[ab], Hongbing Xiao [a], Wenting He [a], Yu Li[a], and Yexiang Tong[b]

[a] *School of Eco-Environmental Technology, Guangdong Industry Polytechnic, 152 Xingang West Road, Guangzhou 510300, China.*

[b] *MOE of the Key Laboratory of Bioinorganic and Synthetic Chemistry, KLGHEI of Environment and Energy Chemistry, School of Chemistry and Chemical Engineering, Sun Yat-Sen University, 135 Xingang West Road, Guangzhou 510275, China.*

**Corresponding Author. E-mail: Qiuwdgq@hotmail.com*

Calculations:

The areal cell capacitances ($C_{cell\text{-}a}$) were calculated from the discharge curve using the following equations:

$$C_{cell-a} = \frac{\int_0^{\Delta t} I \times dt}{S} \quad (1)$$

where I (mA) is the applied discharging current, Δt (h) is the discharging time and S (cm^2) is the area of cell (0.5 cm^2).

Specific capacities ($C_{cell\text{-}s}$) of the cell were estimated from the discharge curve using the following equations:

$$C_{cell-s} = \frac{\int_0^{\Delta t} I \times dt}{m} \quad (2)$$

where $C_{cell\text{-}s}$ (mA h g^{-1}) is the specific capacity of the Ni-Fe battery, I (mA) is the applied discharging current, Δt (h) is the discharging time and m (g) is the mass of the active material of anode and cathode.

Specific energy density E and specific power density P of the cell were obtained from the following equations:

$$E = C_{cell-s} * \Delta V \quad (3)$$

$$P = \frac{C_{cell-s} * \Delta V}{1000 * \Delta t} \quad (4)$$

where E (Wh kg^{-1}) is the energy density, $C_{cell\text{-}s}$ is the specific capacity obtained from Equation (2) and ΔV (V) is the voltage window. P (kW kg^{-1}) is the specific power density and Δt (h) is the discharging time.

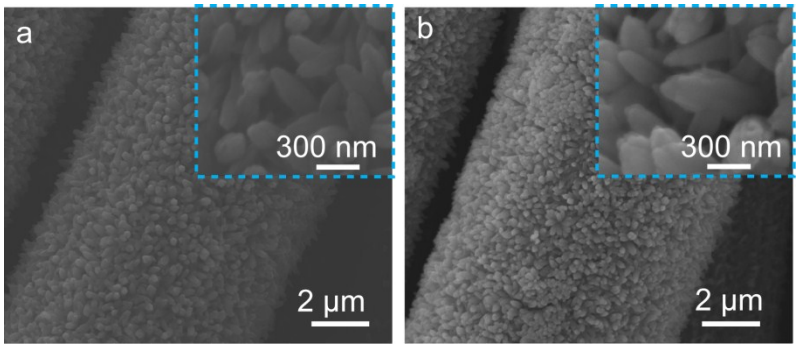

Figure S1. SEM images of the as-prepared FeOOH nanorods (a) and A-Fe_2O_3 nanorods (b).

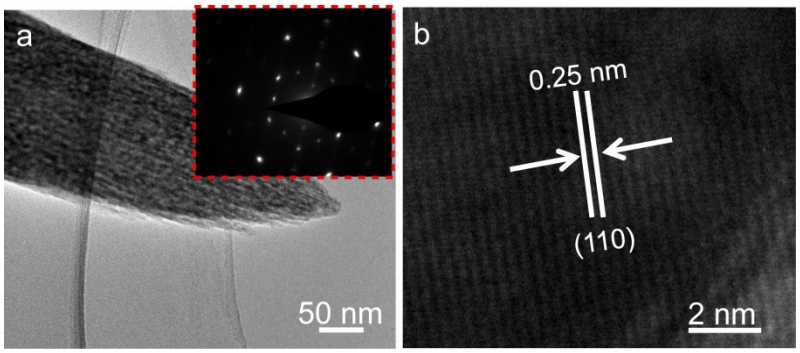

Figure S2. TEM (a) and HRTEM (b) image of the A-Fe_2O_3 nanorods, inset in (a) is the corresponding SAED pattern.

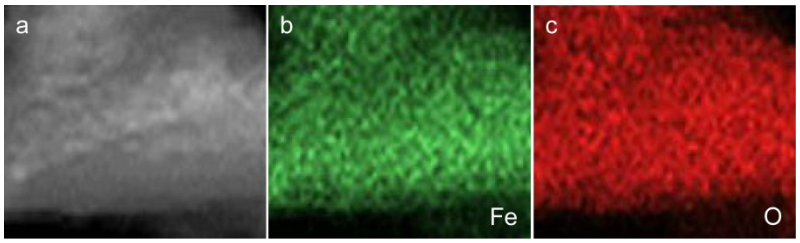

Figure S3. Elemental mapping of the N-Fe_2O_3.

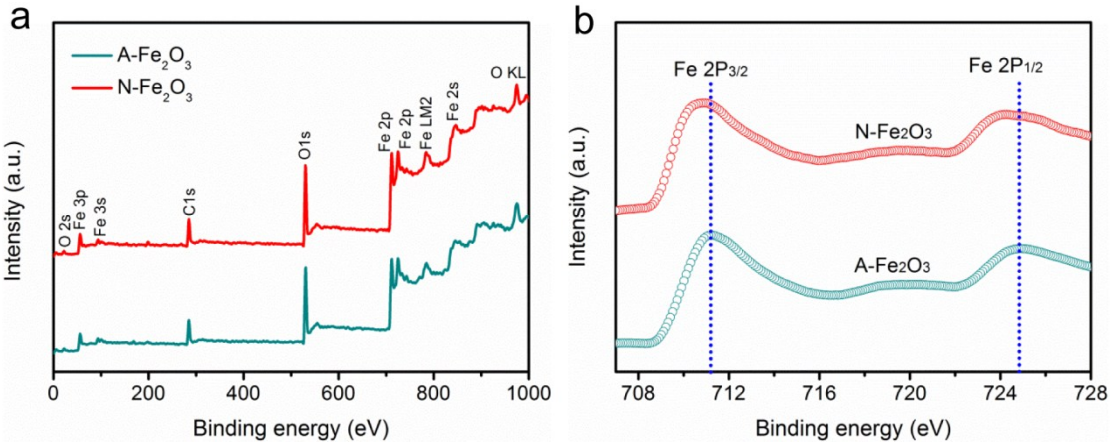

Figure S4. (a) XPS survey and (b) Core level Fe 2p XPS spectra of A-Fe_2O_3 and N-Fe_2O_3 samples.

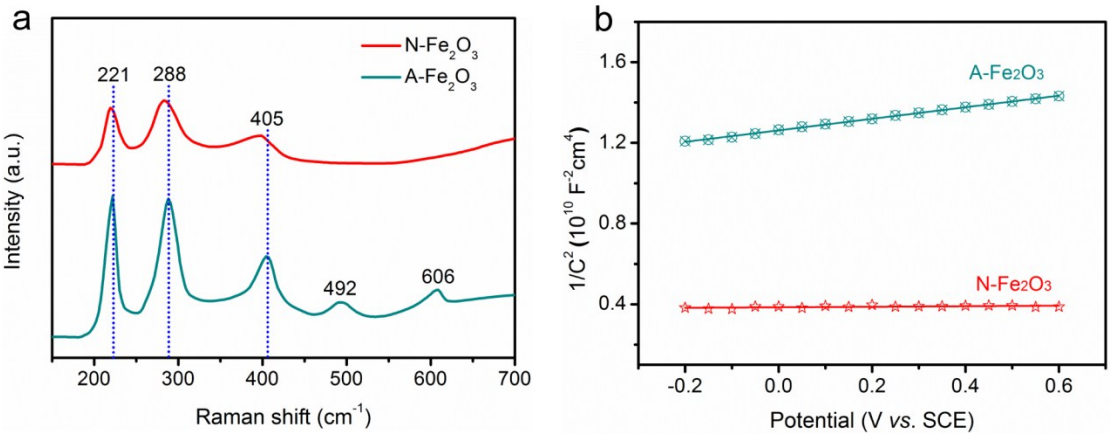

Figure S5. (a) Raman spectra and (b) Mott-Schottky plots of A-Fe_2O_3 and N-Fe_2O_3 samples.

As shown in the Figure S5a, Raman spectra of the two samples can be indexed well to the characteristic Raman peaks of α-Fe_2O_3.[1-3] Comparing with the Raman spectrum of A-Fe_2O_3 sample, the characteristic Raman peaks of N-Fe_2O_3 are negatively shifted and broaden, suggesting the increased amount of oxygen vacancies.[3-5] Furthemore, the

N-Fe_2O_3 sample show substantially smaller slopes of Mott-Schottky plot compared to the A-Fe_2O_3 sample, indicating an increase of donor densities.[2-7] The enhanced donor density is due to the increased oxygen vacancies, which are known to be an electron donor for Fe_2O_3 and improves the conductivity.

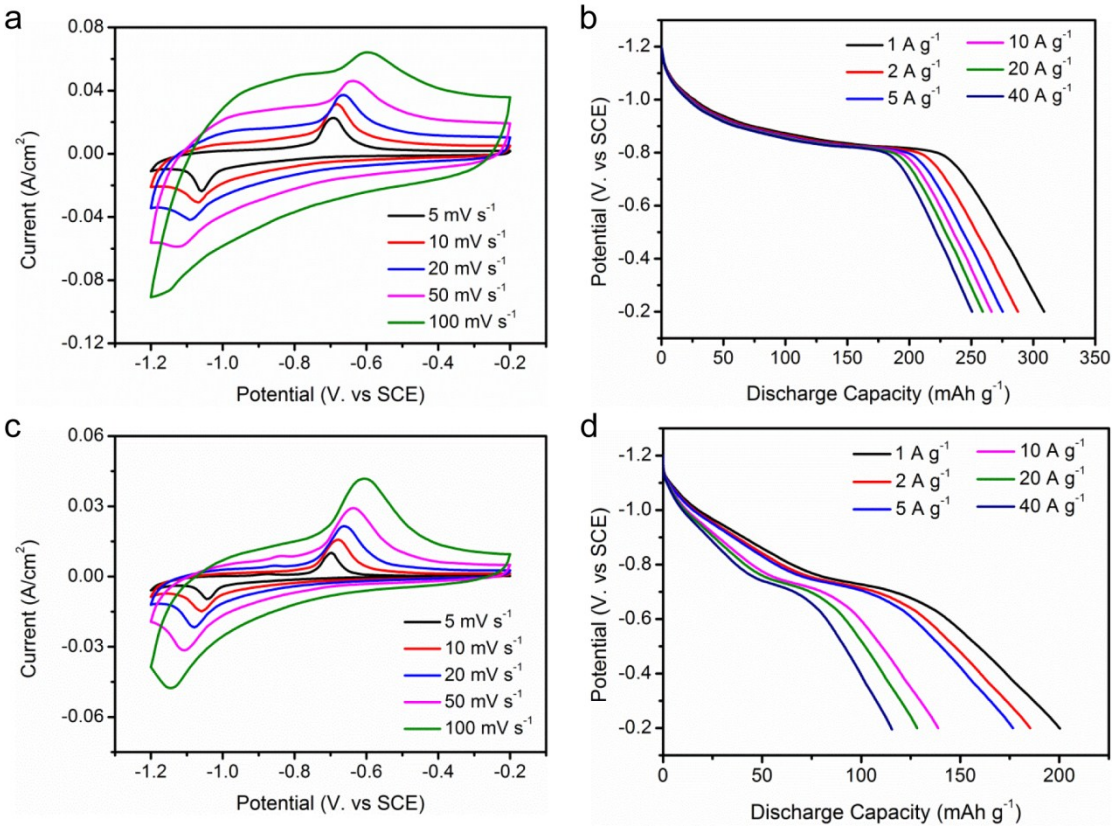

Figure S6. (a) CV curves and (b) charge-discharge curves of the N-Fe_2O_3 samples. (c) CV curves and (d) charge-discharge curves of the A-Fe_2O_3 samples.

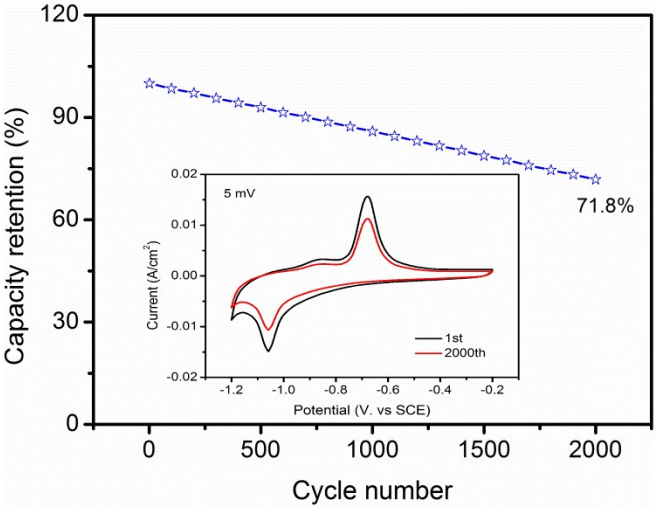

Figure S7. Cycling ability of the A-Fe_2O_3 electrode. Inset is the corresponding CV curves before and after 2000 cycles.

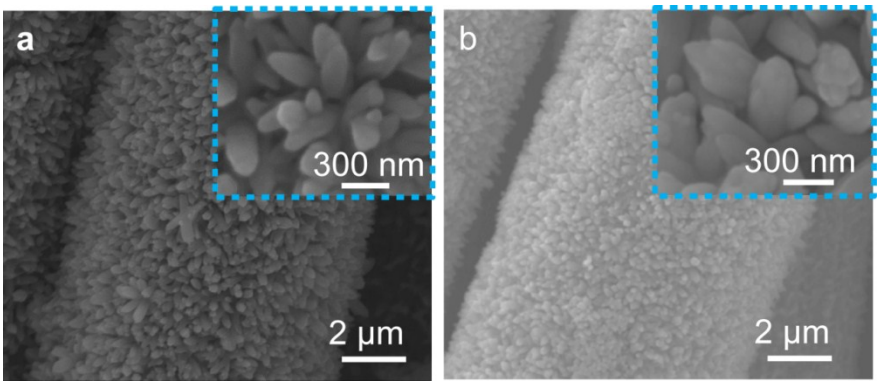

Figure S8. SEM images of as-prepared N-Fe_2O_3 nanorods: (a) before and (b) after 2000 cycles.

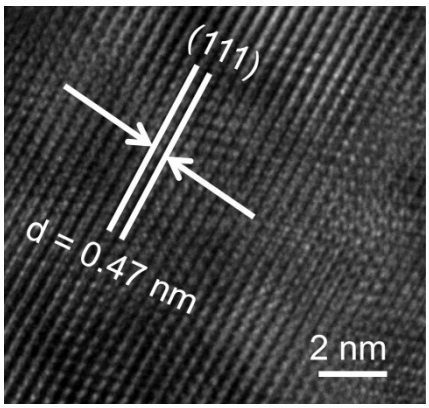

Figure S9. HRTEM image of the P-$NiCo_2O_4$ NWAs.

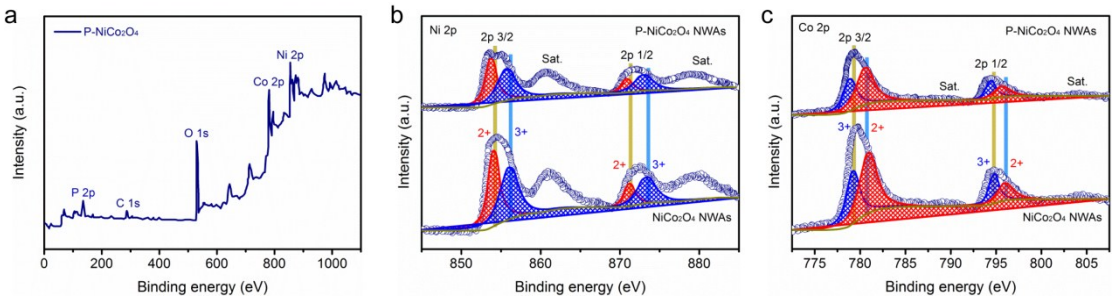

Figure S10. (a) XPS survey spectra of P-$NiCo_2O_4$ NWAs scratched down from carbon cloth. High-resolution XPS spectra (b) Ni 2p, and (c) Co 2p of $NiCo_2O_4$ NWAs and P-$NiCo_2O_4$ NWAs.

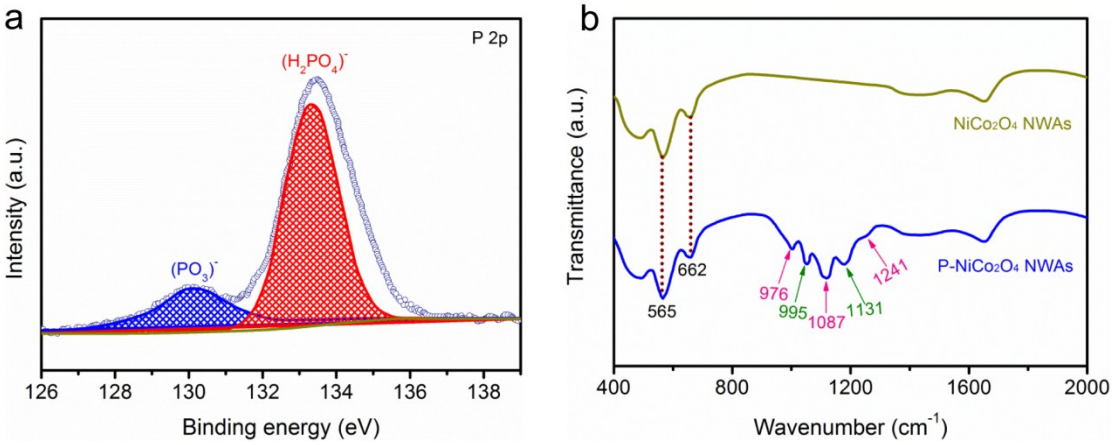

Figure S11. (a) High-resolution XPS spectra of P 2p, (b) FTIR spectra of $NiCo_2O_4$ NWAs and P-$NiCo_2O_4$ NWAs.

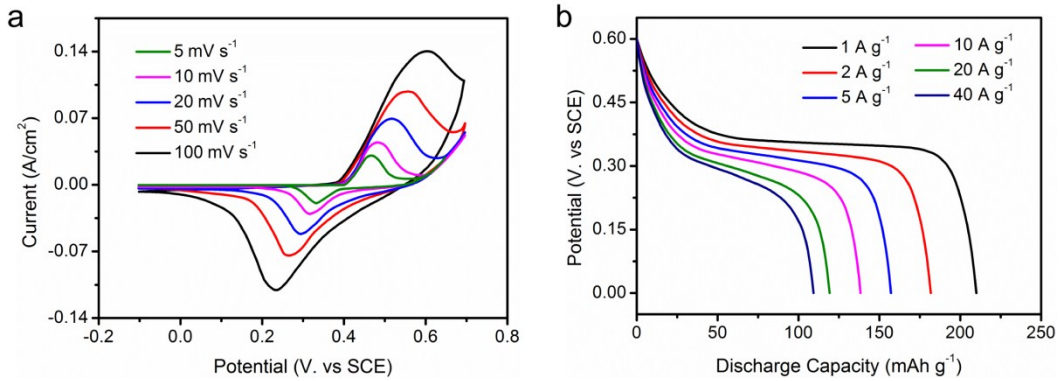

Figure S12. (a) CV curves and (b) discharge curves of $NiCo_2O_4$ NWAs electrode.

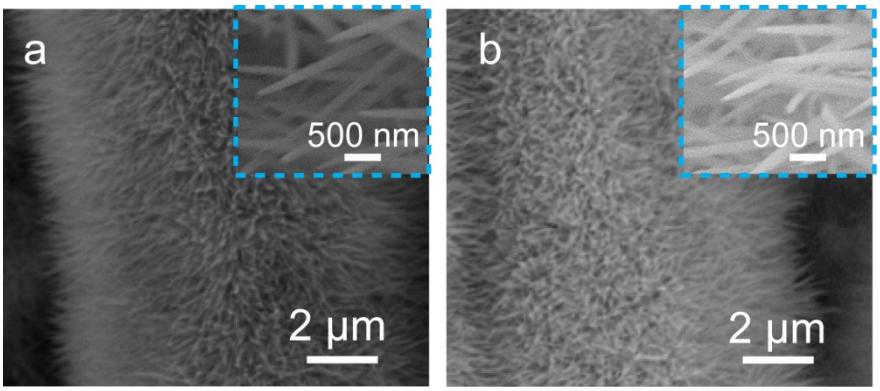

Figure S13. SEM images of as-prepared P-$NiCo_2O_4$ NWAs: (a) before and (b) after 2000 cycles.

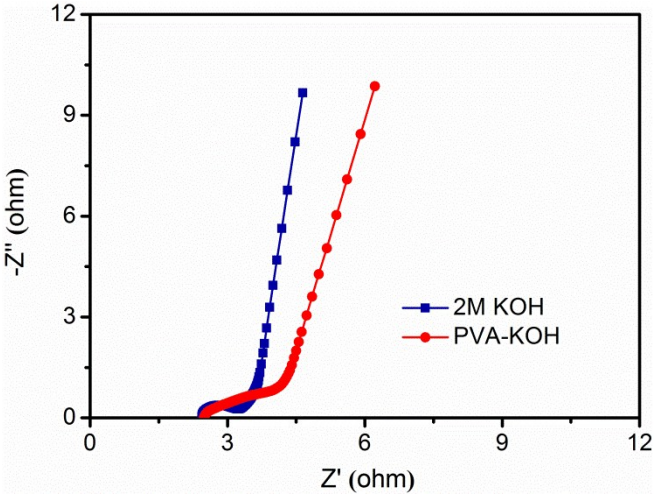

Figure S14. Nyquist plots of the Ni-Fe full cell with different electrolyte.

1. D. De Faria, S. Venâncio Silva and M. De Oliveira, *J. Raman Spectrosc.*, 1997, **28**, 873-878.
2. Y. Ling, G. Wang, J. Reddy, C. Wang, J. Z. Zhang and Y. Li, *Angew. Chem. Int. Ed.*, 2012, **124**, 4150-4155.
3. X. Lu, Y. Zeng, M. Yu, T. Zhai, C. Liang, S. Xie, M. S. Balogun and Y. Tong, *Adv. Mater.*, 2014, **26**, 3148-3155.
4. X. Lu, G. Wang, T. Zhai, M. Yu, J. Gan, Y. Tong and Y. Li, *Nano Lett.*, 2012, **12**, 1690-1696.

5. G. Wang, H. Wang, Y. Ling, Y. Tang, X. Yang, R. C. Fitzmorris, C. Wang, J. Z. Zhang and Y. Li, *Nano Lett.*, 2011, **11**, 3026-3033.
6. Y. Huang, H. Li, M.-S. Balogun, W. Liu, Y. Tong, X. Lu and H. Ji, *ACS Appl. Mater. Interf.*, 2014, **6**, 22920-22927.
7. A. Janotti, J. Varley, P. Rinke, N. Umezawa, G. Kresse and C. Van de Walle, *Phys. Rev. B*, 2010, 81, 085212.